Supporting Information

Two-dimensional Sb@TiO_{2-x} nanoplates as high-performance anode material for sodium-ion batteries

Pengxin Li[a], Xin Guo[b], Shijian Wang[b], Rui Zang[a], Xuemei Li[a], Zengming man[a], Peng Li[a], Shuaishuai Liu[a], Yuhan Wu, Guoxiu Wang[b]*

a College of Material Science and Engineering, Nanjing University of Aeronautics and Astronautics, Nanjing, China

b Centre for Clean Energy Technology, School of Mathematics and Physics, Faculty of Science, University of Technology, Sydney, NSW 2007, Australia

E-mail: *guoxiu.wang@uts.edu.au*

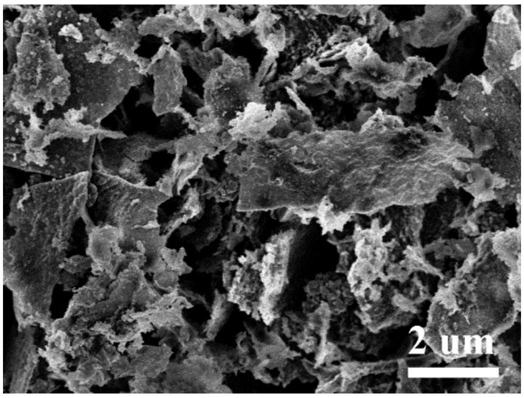

Figure S1 SEM image of the intermediate product after heat treatment in air.

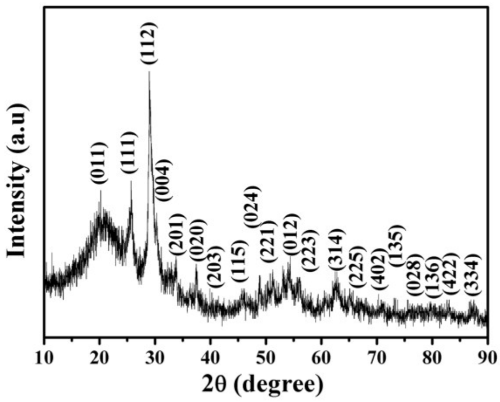

Figure S2 XRD pattern of the intermediate product after heat treatment in air.

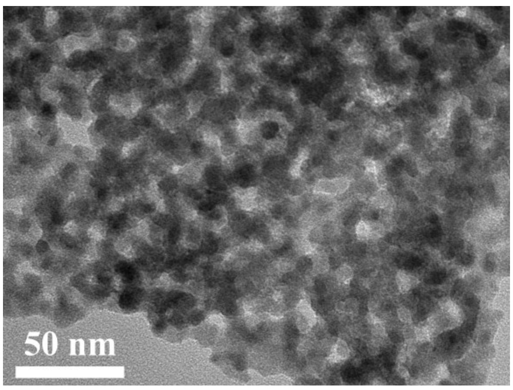

Figure S3 TEM image of the 2D-Sb@TiO_{2-x} nanoplates.

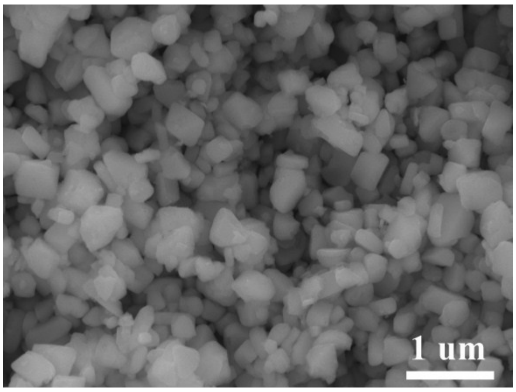

Figure S4 SEM image of the pure Sb material.

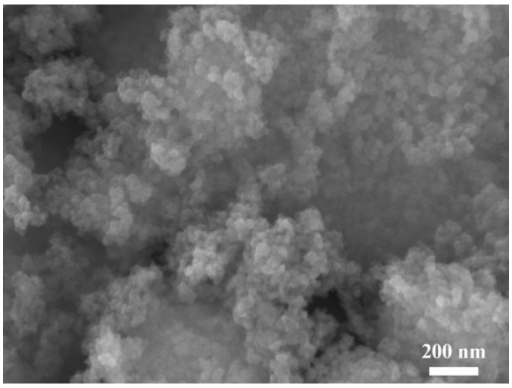

Figure S5 SEM image of the TiO_{2-x} material.

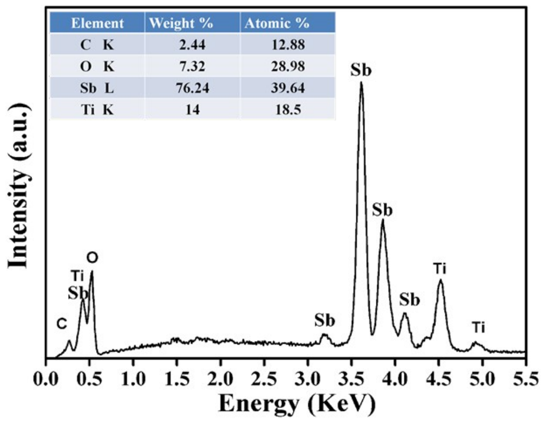

Figure S6 SEM energy dispersive spectroscopic (EDS) characterization and the corresponding quantified element contents (insets) of the 2D-Sb@TiO_{2-x} nanoplates.

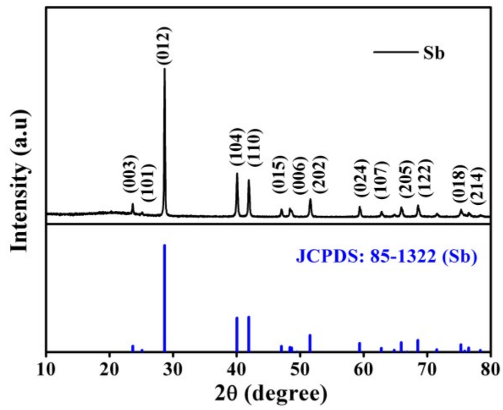

Figure S7 XRD pattern of the pure Sb material.

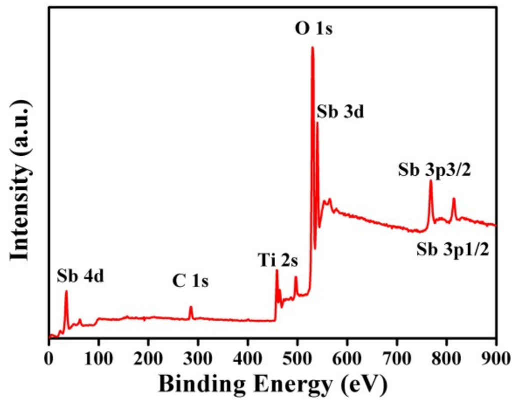

Figure S8 XPS spectrum of the 2D-Sb@TiO_{2-x} nanoplates.

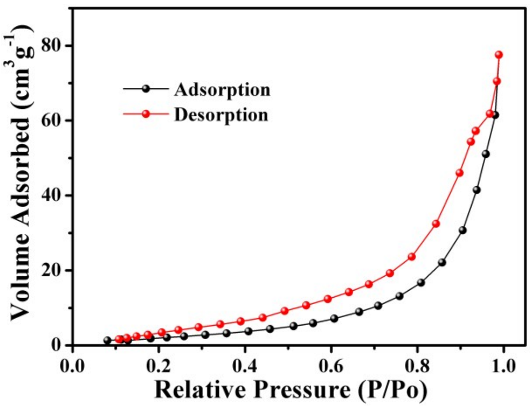

Figure S9 N_2 adsorption/desorption isotherms of the Sb@TiO_{2-x}.

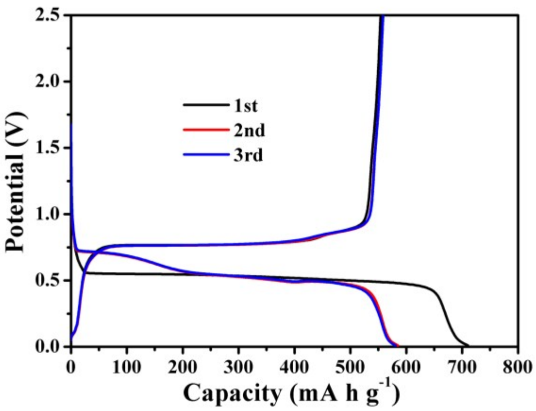

Figure S10 Initial charge and discharge curves of the pure Sb electrode.

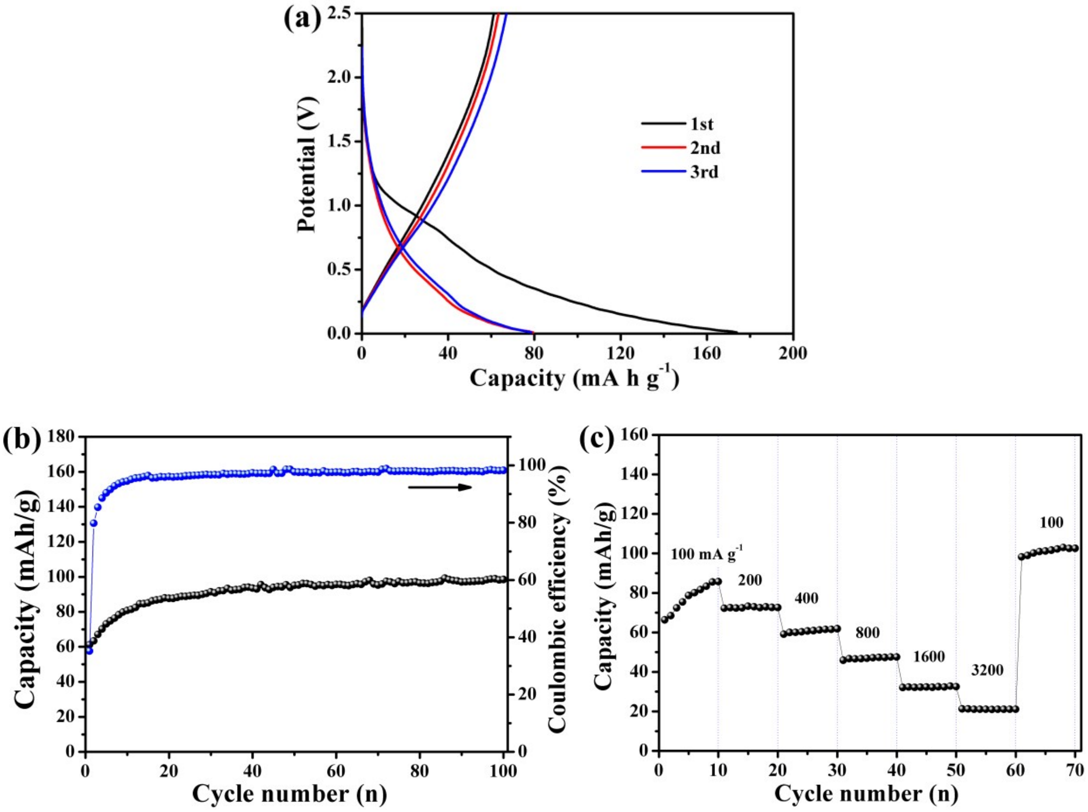

Figure S11 (a) Initial charge and discharge curves of the TiO_{2-x} composite at a current density of 100 mA g^{-1}. (b) Cycling performances of the TiO_{2-x} electrode at 100 mA g^{-1}. (c) Rate performance of the TiO_{2-x} electrode.

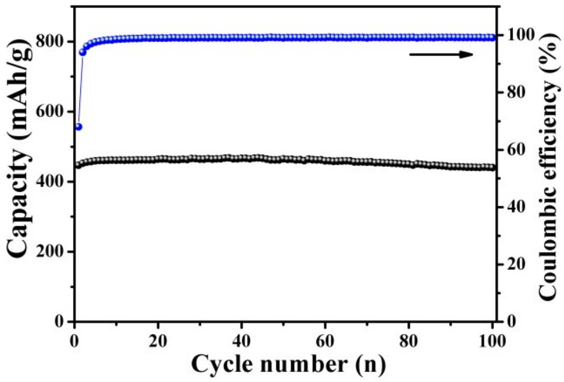

Figure S12 Cycling performances for the 2D-Sb@TiO_{2-x} nanoplates at 1.6 A g^{-1}.

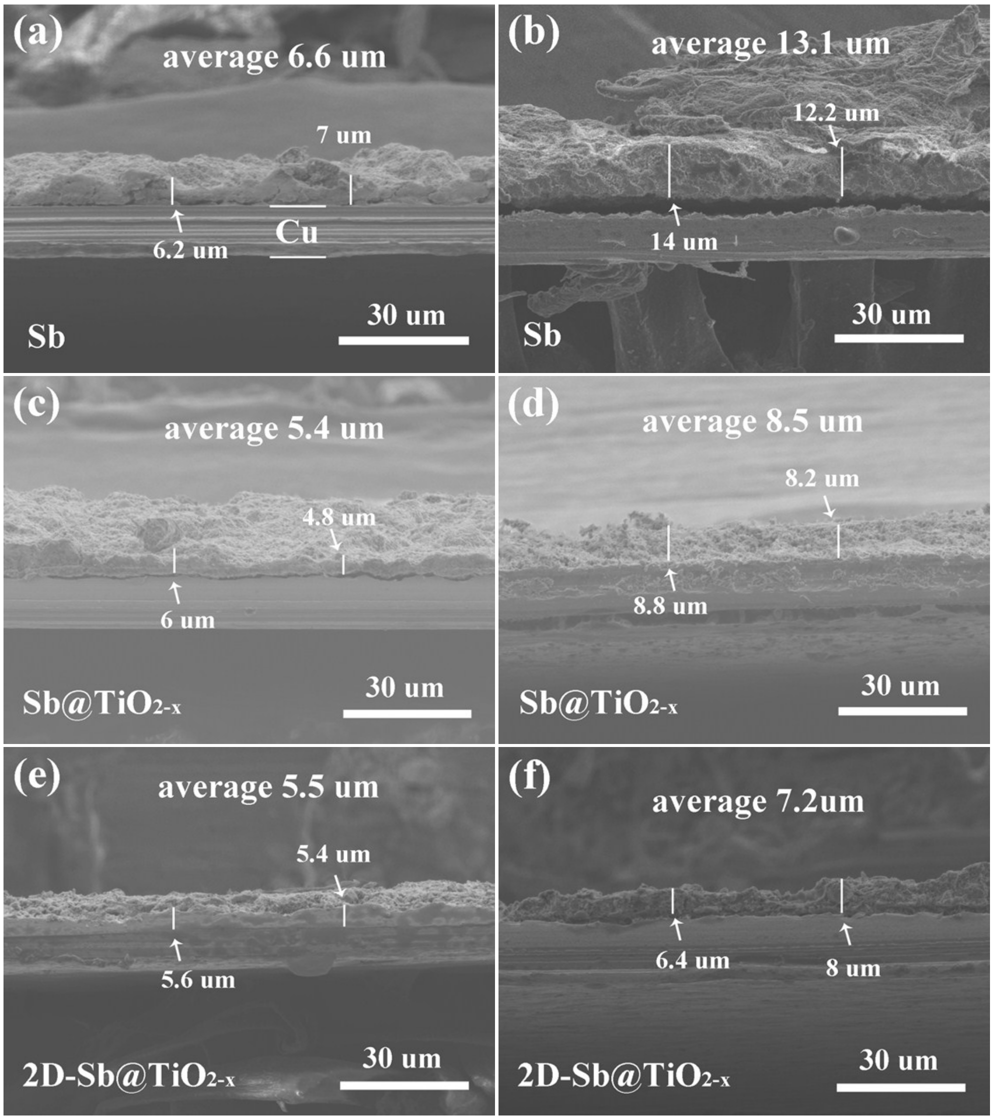

Figure S13 Cross section SEM images of the Sb@TiO_{2-x} and 2D-Sb@TiO_{2-x} electrodes, (a, c and e) original, (b, d and f) post-cycled.

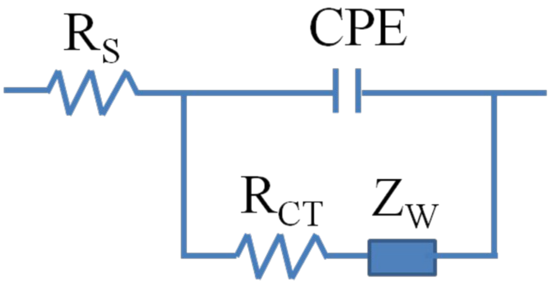

Figure S14 The equivalent circuit model for the fitting of impedance plots. This equivalent circuit model includes an ohmic resistance (R_S), double-layer capacitance (CPE), charge transfer resistance (R_{CT}), and Warburg impedance (Z_W), respectively.

Table S1 The fitting results of charge transfer resistance (R_{CT}) for the 2D-Sb@TiO_{2-x} , Sb@TiO_{2-x}, Sb and TiO_{2-x} from EIS tests.

		2D-Sb@TiO_{2-x}	Sb@TiO_{2-x}	Sb	TiO_{2-x}
R_{CT} (Ω)	5th	83.4	107.8	43.1	186.8
	100th	58.9	130.3	481.8	179

Table S2 Electrochemical performance comparison between the 2D-Sb@TiO_{2-x} nanoplates and the previously reported Sb-based composites.

Materials	Sb content (wt %)	Cycling performance	Rate capability
SbNP@C[1]	54	350 mAh g^{-1} after 300 cycles at 100 mA g^{-1}	88 mAh g^{-1} at 6.0 A g^{-1}
Sb-N/C[2]	15.6	305 mAh g^{-1} after 60 cycles at 50 mA g^{-1}	142 mAh g^{-1} at 10 A g^{-1}
Sb/AB[3]	71.6	473 mAh g^{-1} after 70 cycles at 100 mA g^{-1}	281 mAh g^{-1} at 1.6 A g^{-1}
Sb HNSs[4]	100	622.2 mAh g^{-1} after 50 cycles at 50 mA g^{-1}	315 mAh g^{-1} at 1.6 A g^{-1}
rod-like Sb-C[5]	90.15	430.9 mAh g^{-1} after 100 cycles at 50 mA g^{-1}	259.1 mAh g^{-1} at 0.25 A g^{-1}

Sb/C_{CHI}[6]	40.9	372 mAh g^{-1} after 100 cycles at 500 mA g^{-1}	314 mAh g^{-1} at 4 A g^{-1}
SbNPs@3D-C[7]	31.2	430 mAh g^{-1} after 500 cycles at 100mA g^{-1}	200 mAh g^{-1} at 1.6 A g^{-1}
Sb@NC[8]	62	328 mAh g^{-1} after 300 cycles at 100 A g^{-1}	237 mAh g^{-1} at 5 A g^{-1}
Sb/NPC[9]	57.37	400.9 mAh g^{-1} after 100 cycles at 100 mA g^{-1}	50.4 mAh g^{-1} at 5 A g^{-1}
Sb-CNC[10]	66.5	439 mAh g^{-1} after 150 cycles at 100 mA g^{-1}	302 mAh g^{-1} at 2 A g^{-1}
Sb/TiO_2[11]	80.5	403 mAh g^{-1} after 100 cycles at 100 mA g^{-1}	245 mAh g^{-1} at 2 A g^{-1}
This work	**73.6**	**541 mAh g^{-1} after 100 cycles at 100 mA g^{-1}**	**429 mAh g^{-1} at 3.2 A g^{-1}**

References

1. Y. Zhu, X. Han, Y. Xu, Y. Liu, S. Zheng, K. Xu, L. Hu and C. Wang, *ACS Nano*, 2013, 7, 6378-6386.
2. X. Zhou, Y. Zhong, M. Yang, M. Hu, J. Wei and Z. Zhou, *Chem. Commun.*, 2014, 50, 12888-12891.
3. H. Hou, Y. Yang, Y. Zhu, M. Jing, C. Pan, L. Fang, W. Song, X. Yang and X. Ji, *Electrochimica Acta*, 2014, 146, 328-334.
4. H. Hou, M. Jing, Y. Yang, Y. Zhu, L. Fang, W. Song, C. Pan, X. Yang and X. Ji, *ACS Appl. Mater. Interfaces*, 2014, 6, 16189-16196.
5. L. Fan, J. Zhang, J. Cui, Y. Zhu, J. Liang, L. Wang and Y. Qian, *J. Mater. Chem. A*, 2015, 3, 3276-3280.
6. J. Duan, W. Zhang, C. Wu, Q. Fan, W. Zhang, X. Hu and Y. Huang, *Nano Energy*, 2015, 16, 479-487.
7. W. Luo, P. Zhang, X. Wang, Q. Li, Y. Dong, J. Hua, L. Zhou and L. Mai, *Journal of Power Sources*, 2016, 304, 340-345.
8. X. Xu, Z. Dou, E. Gu, L. Si, X. Zhou and J. Bao, *J. Mater. Chem. A*, 2017, 5, 13411–13420.
9. Q. Q. Yang, J. Zhou, G. Q. Zhang, C. Guo, M. Li, Y. C. Zhu and Y. T. Qian, *J. Mater. Chem. A.*, 2017, 5, 12144-12148.
10. X. Xu, L. Si, X. Zhou, F. Tu, X. Zhu and J. Bao, *Journal of Power Sources*, 2017, 349, 37-44.

11. L. Zhou, Y. Cheng, Q. Sun, L. Sun, C. Wang, X. Wang, D. Yin, L. Wang and J. Ming, Chem. Commun., 2018, 54, 4049-4052.